

Isometric size-scaling of metabolic rate and the size abundance distribution of phytoplankton

María Huete-Ortega, Pedro Cermeño, Alejandra Calvo-Díaz and Emilio Marañón

Proc. R. Soc. B published online 14 December 2011

doi: 10.1098/rsob.2011.2257

Supplementary data

["Data Supplement"](#)

<http://rsob.royalsocietypublishing.org/content/suppl/2011/12/08/rsob.2011.2257.DC1.html>

References

[This article cites 57 articles, 15 of which can be accessed free](#)

<http://rsob.royalsocietypublishing.org/content/early/2011/12/08/rsob.2011.2257.full.html#ref-list-1>

P<P

Published online 14 December 2011 in advance of the print journal.

Email alerting service

Receive free email alerts when new articles cite this article - sign up in the box at the top right-hand corner of the article or click [here](#)

Advance online articles have been peer reviewed and accepted for publication but have not yet appeared in the paper journal (edited, typeset versions may be posted when available prior to final publication). Advance online articles are citable and establish publication priority; they are indexed by PubMed from initial publication. Citations to Advance online articles must include the digital object identifier (DOIs) and date of initial publication.

To subscribe to *Proc. R. Soc. B* go to: <http://rsob.royalsocietypublishing.org/subscriptions>

Isometric size-scaling of metabolic rate and the size abundance distribution of phytoplankton

María Huete-Ortega^{1,*}, Pedro Cermeño¹, Alejandra Calvo-Díaz^{2,†}
and Emilio Marañón¹

¹*Departamento de Ecología y Biología Animal, Universidad de Vigo, Campus Lagoas-Marcosende, 36310 Vigo, Spain*

²*Instituto Español de Oceanografía, Centro Oceanográfico de Xixón, 33212 Xixón, Spain*

The relationship between phytoplankton cell size and abundance has long been known to follow regular, predictable patterns in near steady-state ecosystems, but its origin has remained elusive. To explore the linkage between the size-scaling of metabolic rate and the size abundance distribution of natural phytoplankton communities, we determined simultaneously phytoplankton carbon fixation rates and cell abundance across a cell volume range of over six orders of magnitude in tropical and subtropical waters of the Atlantic Ocean. We found an approximately isometric relationship between carbon fixation rate and cell size (mean slope value: 1.16; range: 1.03–1.32), negating the idea that Kleiber's law is applicable to unicellular autotrophic protists. On the basis of the scaling of individual resource use with cell size, we predicted a reciprocal relationship between the size-scalings of phytoplankton metabolic rate and abundance. This prediction was confirmed by the observed slopes of the relationship between phytoplankton abundance and cell size, which have a mean value of -1.15 (range: -1.29 to -0.97), indicating that the size abundance distribution largely results from the size-scaling of metabolic rate. Our results imply that the total energy processed by carbon fixation is constant along the phytoplankton size spectrum in near steady-state marine ecosystems.

Keywords: phytoplankton size abundance distribution; metabolism; energy use; Kleiber's law; open ocean; carbon fixation rate

1. INTRODUCTION

The size of organisms is a fundamental property that influences individual-level metabolism, community structure and ecosystem functioning [1,2]. Metabolic rates such as carbon fixation, nutrient acquisition or respiration are related to body size by a power function of the form, $M = c V^d$, where M is a metabolic rate, c is a taxon-related constant, V is organism size and d is the size-scaling exponent, which commonly takes a value of approximately $3/4$ [2]. If logarithms are taken, the power function yields the linear relationship, $\log M = \log c + d \log V$, where d is the slope value. Given the pervasiveness of this allometric relationship across taxonomic guilds, trophic levels and biomes, it is generally referred to as Kleiber's law [1,3].

Although previous studies have reported on the applicability of Kleiber's law to marine and freshwater protists [4–6], currently the extent to which this law holds for unicellular organisms is controversial. Recent evidence shows that carbon fixation and respiration rates in eukaryotic unicells scales to cell size with an exponent approximately 1 [7–9]. Normalizing these metabolic rates to cell carbon

mass, the resulting mass-specific rate becomes independent of cell size for organisms spanning more than eight orders of magnitude in size; that is, by analogy with terrestrial vertebrates, elephants in the microbial world may grow as fast as mice do. The only existing determinations of the size-scaling of phytoplankton metabolic rate in natural conditions were obtained by combining independent measurements carried out in many sampling sites [7,10]. However, concurrent determinations of the scaling relationship between phytoplankton metabolic rate and cell size in the field (e.g. in discrete plankton samples of a specific geographical location) are still unavailable, and therefore the variability in the size-scaling exponent is unknown.

Phytoplankton size abundance distribution plays a fundamental role in pelagic ecosystems as it determines the trophic organization of plankton communities and, hence, the biogeochemical functioning of the ecosystem [11,12]. The relationship between phytoplankton abundance and cell size in aquatic ecosystems follows a power function, $N = a V^b$, where N is the cell density and a is the intercept of the resulting linear regression. The size-scaling exponent, b , is a synthetic descriptor of community size structure [2] and generally takes values between -1.3 and -0.6 . The value of the size-scaling exponent is strongly related to ecosystem's productivity. Unproductive ecosystems characteristic of subtropical, oligotrophic regions show steeper slopes (-1.3 to -1.1) [13,14], whereas in coastal, highly productive ecosystems, the slopes become less negative (-0.8 to -0.6), as a result of the increased relative

* Author for correspondence (mhuete@uvigo.es).

† Present addresses: Department of Biological Oceanography, Royal Netherlands Institute for Sea Research (NIOZ), 1790 AB Den Burg, The Netherlands; Department of Marine Biology, University of Vienna, 1090 Vienna, Austria.

Electronic supplementary material is available at <http://dx.doi.org/10.1098/rspb.2011.2257> or via <http://rspb.royalsocietypublishing.org>.

abundance of larger cells [7,15,16]. Despite this connection between ecosystem's productivity and size structure, the origin of the actual values of the size-scaling exponent for phytoplankton cell abundance is still unclear.

The size abundance distribution of organisms within a given ecosystem can be explained as a function of the requirements for limiting resources by the individuals [17,18]. For instance, the relationship between population density and body mass in plants can be derived from the size-scaling of individual resource use such that smaller individuals with lower requirements will attain higher abundances than larger individuals [18]. In the present study, we use the carbon fixation rate as a proxy for metabolic rate and resource use in phytoplankton. We hypothesize that in a nutrient-limited ecosystem, the size-scaling of individual carbon fixation rate controls the size abundance distribution of phytoplankton communities. To test this hypothesis, we analyse concurrently the size-scaling of carbon fixation rate per cell and cell abundance in the tropical and subtropical Atlantic Ocean, a nutrient-impooverished and relatively stable ecosystem close to the steady-state. Our main objectives are (i) to determine, in discrete samples of natural phytoplankton, the scaling relationship between metabolic rate and cell size and (ii) to explore the linkage between the size-scaling of metabolic rate and the size distribution of phytoplankton abundance.

2. METHODS

(a) *Sampling, hydrography, irradiance and nutrients*

We sampled 17 stations during a cruise carried out in November–December 2007 in the tropical and subtropical Atlantic Ocean (figure 1) on board R/V *Hespérides*. At each sampling station, water column hydrography was characterized as described in Huete-Ortega *et al.* [19]. Sampling was conducted before dawn, and different water subsamples were collected from the Niskin bottles to determine nutrient concentration, phytoplankton biomass and abundance, chlorophyll *a* (chl *a*) concentration and primary production. Nanomolar nitrate concentration was determined with a segmented-flow automatic analyser (Technichon/Bran Luebbe), following the method of Raimbault *et al.* [20]. The nitracline depth was defined as the depth below which nitrate concentration was equal to or lower than $0.5 \mu\text{M}$.

(b) *Size-fractionated carbon fixation rate*

Photosynthetic carbon fixation rates were measured with the ^{14}C -uptake technique (for additional details, see Huete-Ortega *et al.* [19]). One litre polycarbonate bottles (one dark and three transparent bottles) were filled with surface (5 m) sea water from each station and, after inoculation with approximately $100 \text{ Bq NaH}^{14}\text{CO}_3$, they were incubated for 6–9 h in on-deck flow-through incubators. At the end of the incubation, water samples were sequentially filtered through $40 \mu\text{m}$ net filters and 20, 10, 5, 3, 2, 0.8 and $0.2 \mu\text{m}$ polycarbonate filters under low vacuum pressure (less than 6.7 mPa). To ensure an adequate representation of larger cells, for 40, 20, 10 and $5 \mu\text{m}$ filters, the whole contents of the 1 l bottles was filtered, whereas in the case of the 3, 2, 0.8 and $0.2 \mu\text{m}$ filters, only 500 ml were filtered. Subsequently, filters were processed to determine the carbon fixation rate of each size class following the procedures described by Maraño *et al.* [21].

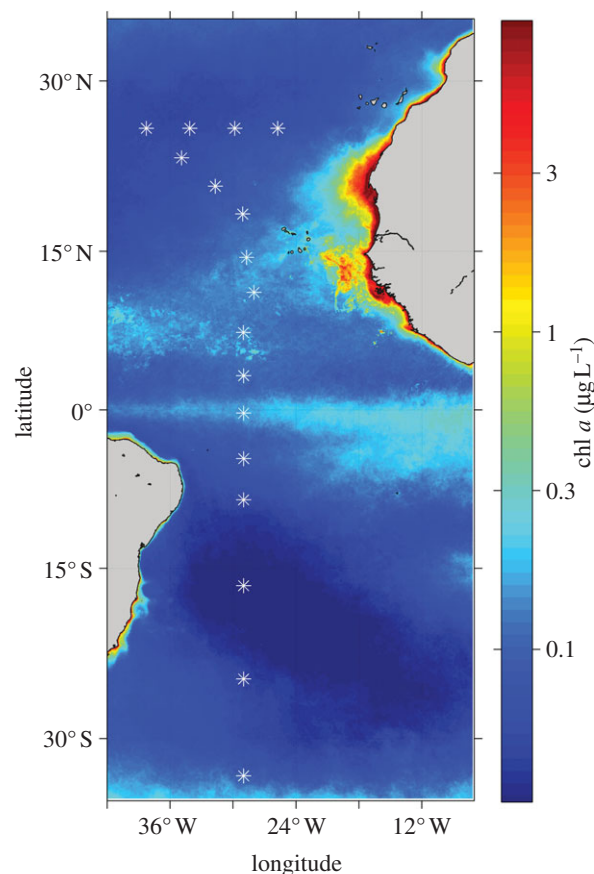


Figure 1. Location of the sampling stations superimposed on a map of the climatological mean surface chlorophyll *a* concentration for the September–November period of the years 2002–2008 in the Atlantic Ocean. Ocean colour data are from MODIS Aqua (9 km).

(c) *Phytoplankton cell size and abundance*

The methods used for determining phytoplankton cell size and abundance have been described in Huete-Ortega *et al.* [19]. To summarize, the abundance of pico- (less than $2 \mu\text{m}$ in equivalent spherical diameter, ESD) and small nanophytoplankton ($2\text{--}5 \mu\text{m}$ in ESD) was determined by flow cytometry using a FACSCalibur flow cytometer (Becton Dickinson), with a laser emitting at 488 nm in frozen samples (4 ml). An empirical calibration between relative side scatter (SSC_{rel}) and cell diameter (D) following Zubkov *et al.* [22] was used to estimate the individual cell biovolume (V) of picophytoplankton cells. For the small nanophytoplankton, V was estimated using a calibration curve that relates the light scattering signal (forward scatter, FSC) to cell biovolume estimated by image analysis [23].

Large nano- ($5\text{--}20 \mu\text{m}$ in ESD) and micro- (greater than $20 \mu\text{m}$ in ESD) phytoplankton were determined by image analysis under an inverted microscope. With the aim of increasing the number of large-sized cells sampled, we used two replicates of 21 of sea water were analysed following the method of Utermöhl [24] and using an Olympus IX50 inverted microscope (more details in Huete-Ortega *et al.* [19] and Zubkov *et al.* [22]). Cell volume was calculated using the geometric shapes recommended in Olenina *et al.* [25].

(d) *Scaling relationship between abundance and cell size*

To determine the scaling relationship between abundance and cell size, size classes were established on an octave (\log_2) scale of biovolume, and total cell abundance was

calculated for each size class by adding the abundance of all cells included in it. Considering that analytical subranges of cell size for flow cytometry and image analysis were approximately 0.5–30 μm ESD and 9–80 μm ESD, respectively, phytoplankton cell abundances from both flow cytometry and microscopy image analysis were coupled for each sample in order to obtain a single size-scaling relationship for the abundance of the whole autotrophic plankton community, from small cyanobacteria to large dinoflagellates and diatoms [23,26]. The maximum number of size classes found was 24, ranging from 0.5 to 80 μm in ESD. Afterwards, the \log_{10} of total abundance was plotted against the \log_{10} of the lower limit of the corresponding octave size class (nominal size) in order to obtain a linear relationship [15,27]. Given that methodological error was present in both variables, the regression slope and the intercept of each size-scaling relationship were calculated using a model II regression analysis by the reduced major-axis (r.m.a) method [28]. Ninety-five per cent confidence intervals (CIs) for the regression parameters were calculated by bootstrapping over cases (2000 repetitions) using the RMA software designed by the San Diego University. When a comparison between slope values was necessary, Student's *t*-test following the Clarke method was used [29].

(e) *Scaling relationship between carbon fixation rate and cell size*

With the aim of determining the size-scaling of photosynthetic carbon fixation rate, total cell abundance was calculated for those size classes for which the size-fractionated carbon fixation rate had been previously obtained (0.2, 0.8, 2, 3, 5, 10, 20 and greater than 40 μm ESD). The size-fractionated carbon fixation rate measured on each size class was divided by the total cell abundance in that size class, thus obtaining the cell-specific carbon fixation rate for each size class. Then the \log_{10} of the cell-specific carbon fixation rate was plotted against the \log_{10} of the corresponding abundance-weighted mean cell size in each size class in order to get a linear relationship [7]. The model II slope and intercept for the carbon fixation versus cell size relationship were calculated using the r.m.a method [28], and the 95% CI for the regression parameters were calculated by bootstrapping over cases (2000 repetitions). The comparison between the obtained slope values and the 3/4 value of Kleiber's law was conducted by the Student's *t*-test following the Clarke method [29].

(f) *Methodological considerations*

Although the size-scaling of phytoplankton carbon fixation has been determined previously in both culture experiments [30] and field studies [7,10], to the best of our knowledge this is the first time that the size-scaling of carbon fixation is determined in natural phytoplankton communities with a high level of accuracy in terms of number of size classes and sample volume used. The small volume of ^{14}C incubations (75–125 ml) normally used for determining primary production in the ocean can result in the undersampling of larger cells, particularly in those ecosystems where they are in lower abundance, such as the oligotrophic gyres [31]. As a result, estimated carbon fixation rates for the large size fractions may be underestimated. In the present study, we applied several modifications in sampling design in order to minimize the underestimation of the abundance and carbon fixation rates of larger cells in the oligotrophic Atlantic Ocean. Specifically, compared with previous studies [7,32], the accuracy of the

size-scaling relationship was improved by increasing substantially the number of size fractions for which carbon fixation rates were estimated (from 3–4 to 8). Also, the 1 l incubations used for the estimation of carbon fixation rates contrasted with the 75–125 ml sample volumes commonly used, thus allowing a better representation of the metabolic rates of larger cells. In addition, the combination of flow cytometry and image analysis enabled us to cover the whole phytoplankton size range, from the smallest cyanobacteria to the largest diatoms. Finally, the potential underestimation of large-sized phytoplankton abundance was also avoided by increasing the sample volume used for image analysis (typically 125 ml) to 2 l.

3. RESULTS

(a) *General oceanographic conditions*

During the cruise, high incident irradiance, warm surface temperature, strong stratification (as evidenced in the low values of the Brunt–Väisälä frequency) and low nutrient concentration in the upper mixed layer (UML) were found throughout the tropical and subtropical Atlantic Ocean (see electronic supplementary material, table S1 and a detailed analysis of hydrographic conditions in Huete-Ortega *et al.* [19]). The influence of the equatorial upwelling could be observed between 17° N and 5° S, where a shallower nitracline depth was found and nitrate concentrations in the UML increased, although without exceeding 0.2 $\mu\text{mol l}^{-1}$ [33]. Nutrient-limited conditions thus prevailed throughout the cruise, and limiting nutrients were supplied to the euphotic layer through small and relatively continuous diffusive fluxes [19]. On the basis of these general oceanographic conditions observed throughout the studied region, a situation close to the steady-state can be assumed, in which nutrients enter the euphotic zone at a slow rate and are continuously consumed by the phytoplankton, so that nutrient concentration never increases markedly.

(b) *Size-scaling of carbon fixation rate*

Figure 2a shows an example of the scaling relationship between cell-specific carbon fixation rate and cell size for a particular community of phytoplankton in the subtropical Atlantic Ocean. For the whole dataset, the size-scaling parameters for cell-specific carbon fixation rate exhibited little variability (figure 3a), with slope values consistently close to, or higher than, 1 (range from 1.03 to 1.32; electronic supplementary material, table S2). These slopes were found to be significantly higher than 0.75 but, with few exceptions, statistically indistinguishable from 1 (Student's *t*-test *p*-values always less than 0.01, electronic supplementary material, table S2). When the size-scaling slopes from all experiments were averaged, the resulting mean slope was 1.16, indicating a slightly superlinear relationship between metabolic rate and cell size. This overall, mean slope value implies that a fourfold increase in cell size would be associated with a fivefold increase in cell-specific carbon fixation rate. This finding was supported by the parallel observation of a nearly isometric relationship between intracellular chl *a* content and cell size (see in electronic supplementary material, figure S3). It is expected that slope values would be even higher than those reported here if the cell size was expressed as carbon units rather than in cell volume, because the power relationship

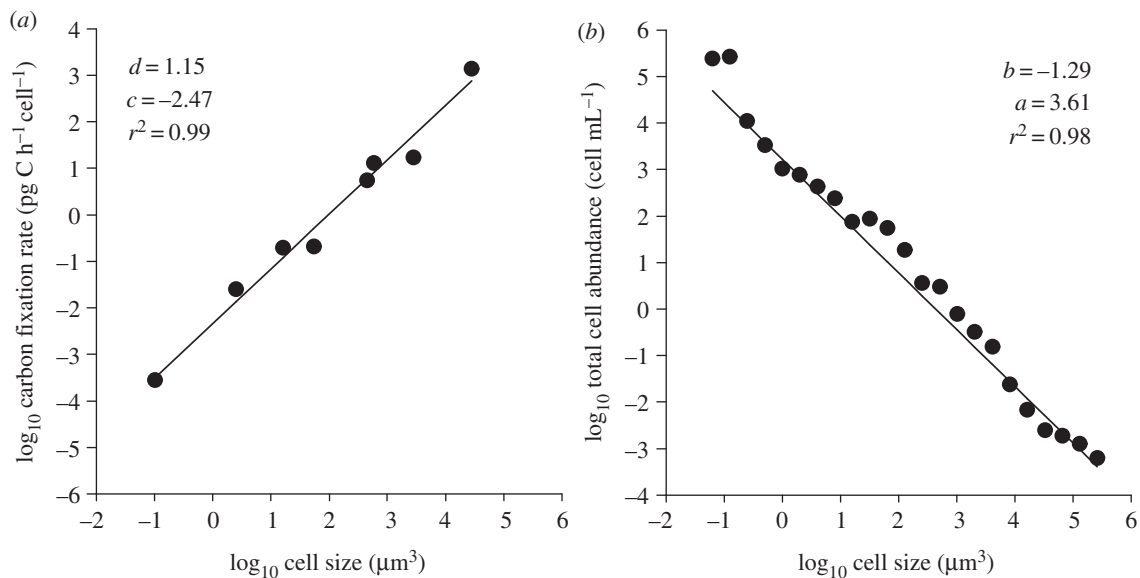


Figure 2. Example of the log–log relationship between (a) cell-specific carbon fixation rate and cell size and (b) total cell abundance and cell size for surface phytoplankton collected at 14.43° N, 28.71° W. d and b are the slope values of the model II regression line, and c and a the corresponding intercept values.

between cell carbon biomass and cell volume often shows an exponent smaller than 1 (see review in [34]).

We assessed the validity of the obtained scaling relationships between carbon fixation rate and cell size by comparing the cell-specific rates predicted for different size classes with species-specific rates reported in the literature and rates estimated in previous size-scaling analysis of phytoplankton photosynthesis. The mean carbon fixation rates determined from our size-scaling relationships for small species such as *Prochlorococcus* spp. and *Synechococcus* spp. (approx. 4×10^{-4} pg C cell⁻¹ h⁻¹ and approx. 1.3×10^{-3} pg C cell⁻¹ h⁻¹, respectively), as well as those obtained for 2 μm ESD picoeukaryotes (approx. 2×10^{-2} pg C cell⁻¹ h⁻¹) and 20 μm ESD microphytoplankton (approx. 58 pg C cell⁻¹ h⁻¹), were all within the range of previous measurements reported for both single species and certain cell size classes in natural phytoplankton assemblages [7,35–37].

(c) *Size-scaling of phytoplankton total abundance*

We observed a consistent, highly significant, inverse linear relationship between phytoplankton total abundance and cell size (see figure 2b for an example of a typical cell size–abundance relationship). Throughout the tropical and subtropical Atlantic Ocean, a high amount of the variability in total phytoplankton abundance was explained by cell size, as r^2 values were always larger than 0.91. The slope of the cell size–abundance relationships ranged between -0.97 and -1.29 (see figure 3b and in electronic supplementary material, table S2 for regression parameters), with a resulting mean slope of -1.15 . These steep slope values coincide with those previously reported for open ocean, oligotrophic ecosystems [7,13,14].

(d) *Size-scaling of phytoplankton total energy use*

Figure 3c shows the scaling relationship between total carbon fixation per unit volume and cell size for each phytoplankton community analysed. This relationship can be

regarded as a proxy for the flow of metabolic energy along the phytoplankton size spectrum. We found that in most cases the regression was not statistically significant; so no size-scaling slopes could be estimated. This result indicates that total energy use by phytoplankton is largely independent of cell size in the oligotrophic Atlantic Ocean.

4. DISCUSSION

(a) *Size-scaling of phytoplankton metabolic rate*

Metabolic rate has long been assumed to follow a 3/4-power relationship with body size in all organisms [1,3,38]. Studies using literature data of metabolic rates had confirmed the applicability of the 3/4-power rule for photosynthetic organisms from the smallest unicellular algae to the largest trees [39,40]. Yet, several experimental studies, focused on unicellular organisms, have recently reported an isometric size-scaling relationship for heat production, respiration and carbon fixation [7–10]. In the present study, all the slopes were significantly higher than the expected value of 3/4, thus constituting another report negating the universal applicability of Kleiber's law [41–43]. This observation implies that biomass-specific carbon fixation rates of large phytoplankton not only are higher than expected for their cell size, but can also be even higher than those of smaller species.

The isometric relationship between respiration and cell size observed in heterotrophic protists has been interpreted as a result of the linear increase in the total volume of mitochondria with cell size [9]. Although a similar reasoning could be applied to the packing of chloroplasts in eukaryotic photoautotrophs, photosynthetic carbon fixation is ultimately constrained by light absorption and nutrient diffusion into the cell, which are both negatively influenced by increasing cell size through the package effect and changes in the surface-to-volume ratio [30,44,45]. Therefore, we hypothesize that other physiological and/or ecological strategies in addition to those proposed for respiratory rates in unicellular protists must be invoked to explain the isometric

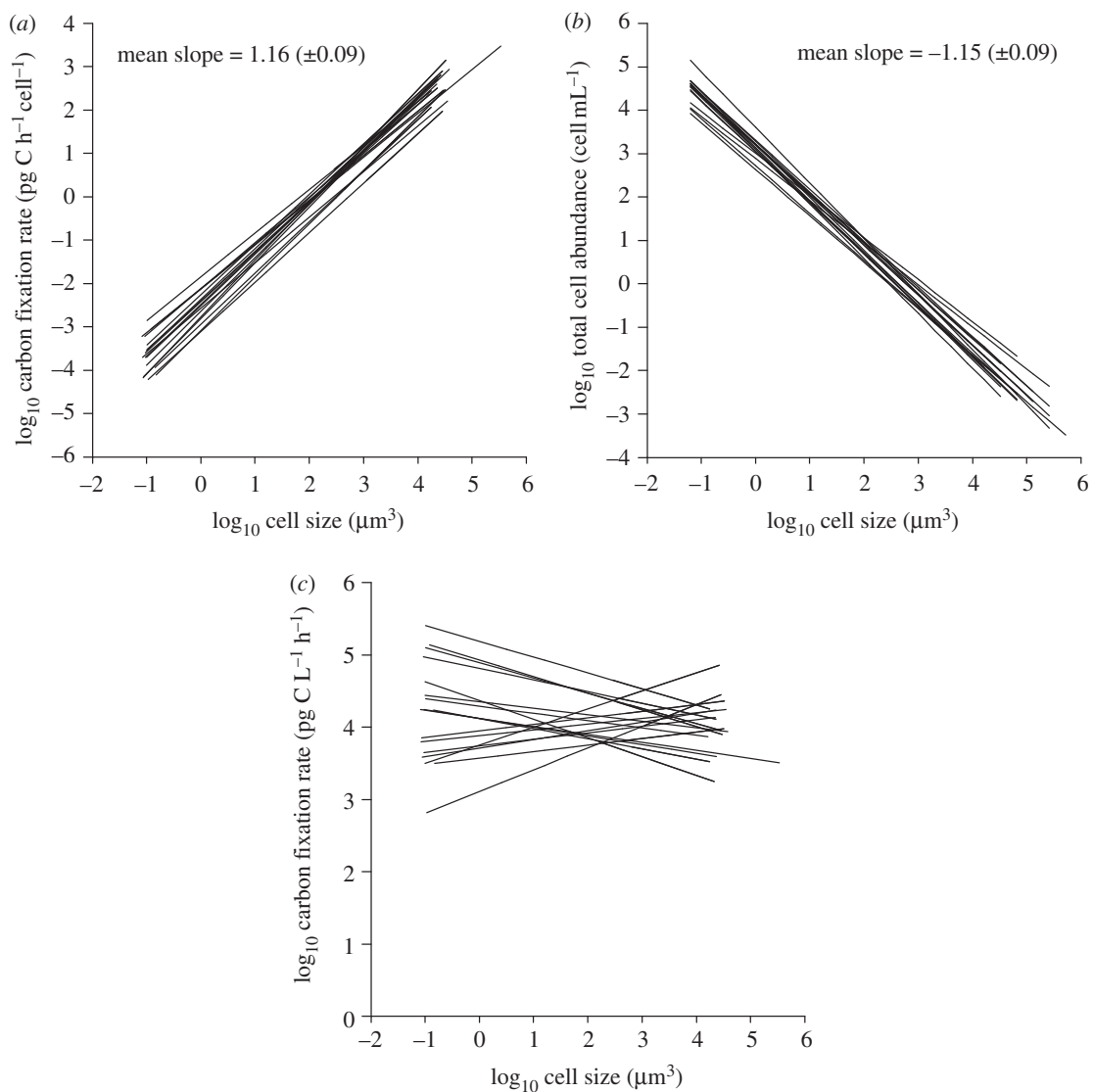


Figure 3. Best fit to data for the log–log relationships between (a) cell-specific carbon fixation rate and cell size, (b) total cell abundance and cell size as well as (c) total carbon fixation rate per unit volume and cell size in all samples obtained during the cruise. Regression parameters for each size-scaling relationship are detailed electronic supplementary material, table S2. Slope values in (a) and (b) refer to the mean (\pm s.d.) slope for each type of size-scaling relationship, which was obtained by averaging the size-scaling slopes from all the experiments.

scaling relationship between phytoplankton carbon fixation rate and cell size.

Microalgal species must maximize their resource acquisition and assimilation rates while minimizing loss rates in order to survive in aquatic pelagic ecosystems [46]. Thus, the size-scaling relationships in phytoplankton might have evolved, in part, as a consequence of adaptation processes that involved the acquisition of taxa-specific physiological strategies by species in certain size classes [47]. For instance, a number of structural and biophysical features of large phytoplankton may counterbalance their geometric constraints on resources acquisition, which otherwise favour small cells when resources are limiting [45,48]. These traits include the possession of intracellular vacuoles to increase nutrient storage capacity [47,49], changes in cell shape [50,51], the use of non-limiting substrates to increase cell size without increasing nutrient requirements [52], the ability to migrate vertically in the water column [53] and the establishment of associations with nitrogen fixers [54].

(b) Linking the size-scaling of phytoplankton metabolism and abundance

The size abundance distribution of phytoplankton communities in near steady-state ecosystems can be explained as a function of the supply rate (R) of limiting nutrients and the rate of nutrient use per individual (Q), so that $N = R/Q$ [18,55]. Given that photosynthetic carbon fixation in surface phytoplankton of low latitudes, where incident irradiance is high, is largely dependent on nutrient availability, we can use the analysis of its scaling along the size spectrum to assess the size-scaling of nutrient use (Q) by phytoplankton. Thus, we take d , the slope of the scaling relationship between cell-specific carbon fixation rate and cell size, as the size-scaling exponent for the individual rate of nutrient use, so that $Q \propto V^d$. Larger cells have higher nutrient requirements (or metabolic rates) and thus, for a given amount of limiting nutrients, will attain lower population densities than their smaller counterparts. Therefore, assuming that limiting nutrients were equally available along the phytoplankton size spectrum ($R \propto V^0$),

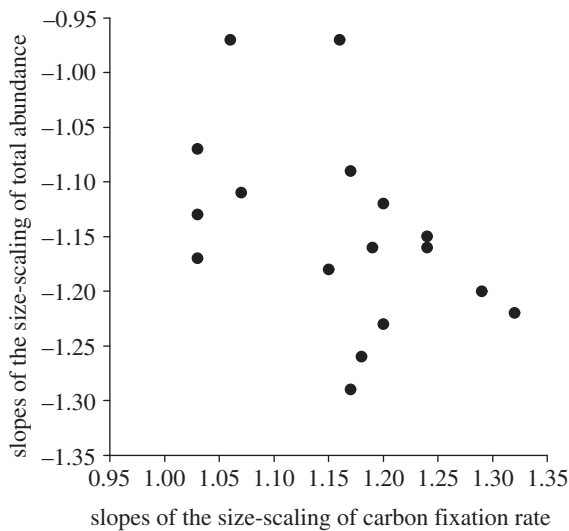


Figure 4. Relationship between the slopes of the size-scaling of cell-specific carbon fixation rate (CF) and total cell abundance (TA) obtained for the tropical and subtropical Atlantic Ocean (see electronic supplementary material, table S2 for more details). The model II regression line is: ‘TA slope = 0.13 (−0.53, 0.85)—1.09 (−1.70, −0.55) CF slope’ ($r^2 = 0.20$, p -value = 0.078, $n = 17$), with 95% confidence intervals for each regression parameter given between brackets. Note that the size-scaling slopes for both variables range between 1 and 1.3 in absolute values, indicating reciprocity between the size-scaling of abundance and metabolic rate.

we predict that the size-scaling exponent for cell abundance, b , will take the same value as the size-scaling exponent of carbon fixation (metabolic rate), but with opposite sign, as $N \propto V^0/V^d = V^{-d}$; a situation that is referred as the reciprocal size-scaling of metabolic rate and abundance. On average, in our study the slope of the relationship between carbon fixation rate per individual and cell size was 1.16 (figure 3a). Then, according to the earlier mentioned model, the size-scaling relationship of phytoplankton abundance is predicted to take a slope of -1.16 , which is strikingly similar to -1.15 (Student’s t -test p -value < 0.01), the mean slope of all the scaling relationships between abundance and cell size obtained throughout the study region (figure 3b). This reciprocal relationship is also supported by the negative relationship found between the size-scaling slopes of cell-specific carbon fixation rate and total abundance (p -value = 0.078, $r^2 = 0.20$, figure 4). We thus conclude that over broad scales the size-scaling of phytoplankton abundance in open ocean ecosystems near to steady-state, with slopes typically ranging between -1 and -1.3 , can be explained as a direct consequence of the size-scaling of phytoplankton metabolic rate.

The simultaneous knowledge of the size-scaling of phytoplankton metabolism and cell abundance allows us to study the flow of energy along the size spectrum [7]. Damuth’s theory states that the total energy used by a given species population per unit area (EU) can be assessed by multiplying the average energy use per individual (or resource use, Q) and the abundance of the individuals (N) [17]. Even though in the present study there was no differentiation of species composition, in practice each size class was an assemblage of species. Accordingly, the reciprocal relationship found between

the size-scalings of carbon fixation rate per individual (metabolic rate) and cell abundance (mean slope values in figure 3a,b, respectively, $Q \propto V^{1.16}$ and $N \propto V^{-1.15}$) would yield the invariance with respect to the cell size of the total energy use by phytoplankton, as $EU \propto V^{1.16-1.15} = V^{0.01}$. As we can see in figure 3c, no significant regression relationships were found between phytoplankton total carbon fixation rates and cell size throughout the study region, thus confirming that in an open ocean, near steady-state ecosystem such as the central tropical and subtropical Atlantic Ocean, total energy processed by phytoplankton metabolism is the same in all of the size spectrum. This conclusion contrasts with that of Li *et al.* [56], who hypothesized a dominance of total energy use by small phytoplankton in oligotrophic oceanic regions. However, this study assumed that phytoplankton metabolic rate follows a 3/4-power relationship with cell size, without conducting any *in situ* measurements of size-fractionated phytoplankton metabolic rates. The observed invariance of the total energy use along the size spectrum implies that, contrary to conventional wisdom, primary production of large-sized phytoplankton is largely equal to that estimated for smaller cells in the oligotrophic, near steady-state ecosystems of the open ocean. This result may be explained by the methodological improvements carried out in the present study, as it seems that the small-volume incubations commonly conducted for estimating open ocean primary production might be underestimating the carbon fixation rates of larger fractions (see electronic supplementary material, figure S4). If confirmed, the underestimation observed and the subsequent size-independence of total energy use can have important implications for global carbon budgets, including the balance between photosynthesis and mesopelagic respiration [57].

The conceptual linkage between the size-scaling of metabolic rate and the size abundance distribution of phytoplankton communities explored here is valid only in near steady-state marine ecosystems, where nutrients enter the euphotic layer through small and relatively continuous diffusive fluxes from below the thermocline, and metabolic rates are nutrient-limited [18]. In these settings, the availability of limiting nutrients will be uniformly distributed along the size spectrum; so all individuals within a given size class will have equal access to their corresponding limiting nutrient and will grow until reaching the cell abundance that corresponds to their rate of nutrient use, in turn determined by their cell size. This explains the seemingly paradoxical fact that, while larger cells have higher biomass-specific carbon fixation rates, they attain lower abundances than their smaller counterparts, rather than dominating the phytoplankton community. In this sense, higher biomass-specific carbon fixation rates of large phytoplankton imply higher nutrient requirements and thus, in near steady-state marine ecosystems, the limited amount of nutrients will have to be shared by a smaller number of larger cells. Other processes such as size-differential grazing pressure by zooplankton [58] may affect the regular patterns in size abundance distribution of marine phytoplankton, by controlling phytoplankton abundances along the size spectrum and preventing the development of blooms of certain phytoplankton size groups. However, in marine ecosystems near to steady-state, grazing pressure is higher on small phytoplankton and the losses of smaller

cells may be compensated by the higher sedimentation rates experienced by larger cells [11,46,59], resulting in a broad cell size-independence of loss processes. Furthermore, it has been hypothesized that resource competition between phytoplankton species of different size should lead to the dominance of phytoplankton community by the single size that requires the lowest resource concentration to grow [47,48]. However, here we assume that, given that different phytoplankton species have different nutrient requirements and phytoplankton taxonomic composition changes with cell size [60,61], the nature of the limiting nutrient may vary along the size spectrum. This fact, together with the effect of dispersion and episodic changes in resource supply, may prevent the establishment of competitive exclusion between different size classes. Therefore, the overall slope of the size–abundance spectrum will be ultimately determined by the rate of nutrient supply and its use by phytoplankton, while the concurrent influence along the size spectrum of other ecological mechanisms contributes to the observed variability among the abundance size-scaling relationships around an average isometric scaling.

5. CONCLUSIONS

We have confirmed, using *in situ* measurements of photosynthetic carbon fixation in local, natural assemblages, that the 3/4-power law is not applicable to phytoplankton metabolism in the field, thus negating the universality of Kleiber's rule. The isometric size-scaling of phytoplankton carbon fixation is likely to result from taxa-specific physiological strategies of larger species, which allow them to overcome the size-related constraints on resource uptake and use. The inverse power–law relationship between phytoplankton abundance and cell size, with exponents typically between -1 and -1.3 , is a well-established property of near steady-state open ocean ecosystems; yet, its origin has remained elusive. The concurrent analysis of the relationship between cell size and phytoplankton abundance and photosynthetic carbon fixation rate suggests that the observed size abundance distribution in these ecosystems arises as a direct result of the size-scaling of metabolic rate. As a consequence of the reciprocal relationship found between the size-scalings of metabolic rate per individual and cell abundance, total energy use by phytoplankton metabolism is invariant along the size spectrum in the tropical and subtropical Atlantic Ocean. From a biogeochemical standpoint, this invariance highlights the importance of large phytoplankton productivity in oligotrophic, near steady-state ecosystems of the open ocean, where the role of this size class in carbon budgets has been so far undervalued.

We thank J. Escánez and F. J. Domínguez for the nutrient data and L. Díaz and P. Chouciño for their support in the analysis of flow cytometry and chl *a* samples, respectively. We are also grateful to D. López-Sandoval for her help with figure 1. We acknowledge the support of the officers and crew of the R/V *Hespérides*, as well as the staff of the Marine Technology Unit (UTM), during the work at sea. Comments from two anonymous reviewers are also gratefully acknowledged. M.H.-O. and A.C.-D. were supported by undergraduate fellowships from the Spanish Ministry of Education. P.C. was supported by Marie Curie Outgoing International Fellowship within the 6th European Community framework Programme. This research was funded by Spanish Ministry

of Science and Innovation through grants CTM2004-05174-C02 (*Trichodesmium* and N_2 fixation in the tropical Atlantic) and CTM2008-03699 (Macroecological patterns in marine phytoplankton) to E.M.

REFERENCES

- Peters, R. H. 1983 *The ecological implications of body size*, 1st edn. Cambridge, UK: Cambridge University Press.
- Marquet, P. A., Quiñones, R. A., Abades, S., Labra, F., Tognelli, M., Arim, M. & Rivadeneira, M. 2005 Scaling and power-laws in ecological systems. *J. Exp. Biol.* **208**, 1749–1769. (doi:10.1242/jeb.01588)
- Kleiber, M. 1947 Body size and metabolic rate. *Physiol. Rev.* **27**, 511–541.
- Taguchi, S. 1976 Relationship between photosynthesis and cell size of marine diatoms. *J. Phycol.* **12**, 185–189. (doi:10.1111/j.1529-8817.1976.tb00499.x)
- Nielsen, S. L. & Sand-Jensen, K. 1990 Allometric scaling of maximal photosynthetic growth rate to surface/volume ratio. *Limnol. Oceanogr.* **35**, 177–181. (doi:10.4319/lo.1990.35.1.0177)
- López-Urrutia, A., San Martín, E., Harris, R. P. & Irigoien, X. 2006 Scaling the metabolic balance of the oceans. *Proc. Natl Acad. Sci. USA* **103**, 8739–8744. (doi:10.1073/pnas.0601137103)
- Marañón, E., Cermeño, P., Rodríguez, J., Zubkov, M. V. & Harris, H. P. 2007 Scaling of phytoplankton photosynthesis and cell size in the ocean. *Limnol. Oceanogr.* **52**, 2190–2198. (doi:10.4319/lo.2007.52.5.2190)
- Johnson, M. D., Völker, J., Moeller, H. V., Laws, E., Breslauer, K. J. & Falkowski, P. G. 2009 Universal constant for heat production in protists. *Proc. Natl Acad. Sci. USA* **106**, 6696–6699. (doi:10.1073/pnas.0902005106)
- DeLong, J. P., Okie, J. G., Moses, M. E., Sibly, R. M. & Brown, J. H. 2010 Shifts in metabolic scaling, production, and efficiency across major evolutionary transitions of life. *Proc. Natl Acad. Sci. USA* **107**, 12 941–12 945. (doi:10.1073/pnas.1007783107)
- Marañón, E. 2008 Inter-specific scaling of phytoplankton production and cell size in natural ecosystems. *J. Plankton Res.* **30**, 157–163. (doi:10.1093/plankt/fbm087)
- Kjørboe, T. 1993 Turbulence, phytoplankton cell size, and the structure of pelagic food webs. *Adv. Mar. Biol.* **29**, 1–72. (doi:10.1016/S0065-2881(08)60129-7)
- Legendre, L. & Rassoulzadegan, F. 1996 Food-web mediated export of biogenic carbon in oceans: hydrodynamic control. *Mar. Ecol. Prog. Ser.* **145**, 179–193. (doi:10.3354/meps145179)
- Cavender-Bares, K., Rinaldo, A. & Chisholm, S. W. 2001 Microbial size spectra from natural and nutrient enriched ecosystems. *Limnol. Oceanogr.* **46**, 778–789. (doi:10.4319/lo.2001.46.4.0778)
- Cermeño, P. & Figueiras, F. G. 2008 Species richness and cell-size distribution: the size structure of phytoplankton communities. *Mar. Ecol. Prog. Ser.* **357**, 79–85. (doi:10.3354/meps07293)
- Reul, A., Rodríguez, V., Jiménez-Gómez, F., Blanco, J. M., Bautista, B., Sarhan, T., Guerrero, F., Ruiz, J. & García-Lafuente, J. 2005 Variability in the spatio-temporal distribution and size-structure of phytoplankton across an upwelling area in the NW-Alboran Sea, (W-Mediterranean). *Cont. Shelf Res.* **25**, 589–608. (doi:10.1016/j.csr.2004.09.016)
- Huete-Ortega, M., Marañón, E., Varela, M. & Bode, A. 2010 General patterns in the size scaling of phytoplankton abundance in coastal waters during a 10-year time series. *J. Plankton Res.* **32**, 1–14. (doi:10.1093/plankt/fbp104)
- Damuth, J. 1981 Population density and body size in mammals. *Nature* **290**, 699–700. (doi:10.1038/290699a0)

- 18 Enquist, B. J., Brown, J. H. & West, G. B. 1998 Allometric scaling of plant energetics and population density. *Nature* **395**, 163–165. (doi:10.1038/25977)
- 19 Huete-Ortega, M., Calvo-Díaz, A., Graña, R., Mouriño-Carballido, B. & Marañón, E. 2011 Effect of environmental forcing on the biomass, production and growth rate of size-fractionated phytoplankton in the central Atlantic Ocean. *J. Mar. Syst.* **88**, 203–213. (doi:10.1016/j.jmarsys.2011.04.007)
- 20 Raimbault, P., Rodier, M. & Taupier-Letage, I. 1988 Size fraction of phytoplankton in the Ligurian Sea and the Algerian Basin (Mediterranean Sea): size distribution versus total concentration. *Mar. Microb. Food-Webs* **3**, 1–7.
- 21 Marañón, E., Holligan, P. M., Barciela, R., González, N., Mouriño, B., Pazó, M. J. & Varela, M. 2001 Patterns of phytoplankton size-structure and productivity in contrasting open ocean environments. *Mar. Ecol. Prog. Ser.* **216**, 43–56. (doi:10.3354/meps216043)
- 22 Zubkov, M. V., Sleight, M. A., Tarran, G. A., Burkill, P. H. & Leakey, R. J. G. 1998 Picoplanktonic community structure on an Atlantic transect from 50° N to 50° S. *Deep-Sea Res. I* **45**, 1339–1355. (doi:10.1016/j.csr.2004.09.016)
- 23 Rodríguez, J., Blanco, J. M., Jiménez, F., Echevarría, F., Gil, J., Rodríguez, V., Ruíz, J., Bautista, B. & Guerrero, F. 1998 Patterns in the size structure of the phytoplankton community in the deep fluorescence maximum of the Alboran Sea (southwestern Mediterranean). *Deep-Sea Res. I* **45**, 1577–1593. (doi:10.1016/S0967-0637(98)00030-2)
- 24 Lund, J. W. G., Kipling, C. & Le Cren, E. D. 1958 The inverted microscope method of estimating algal numbers and the statistical basis of estimations by counting. *Hydrobiologia* **11**, 143–170. (doi:10.1007/BF00007865)
- 25 Olenina, I. *et al.* 2006 Biovolumes and size-classes of phytoplankton in the Baltic Sea. In *Baltic Sea Environment Proceedings*, vol. 106, pp. 144. Helsinki: Helsinki Commission and Baltic Marine Environment Commission.
- 26 Rodríguez, J., Jiménez-Gómez, F., Blanco, J. M. & Figueroa, F. L. 2002 Physical gradients and spatial variability of the size structure and composition of phytoplankton in the Gerlache Strait (Antarctica). *Deep-Sea Res. II* **49**, 693–706. (doi:10.1016/S0967-0645(01)00119-9)
- 27 Blanco, J. M., Echevarría, F. & García, C. M. 1994 Dealing with size spectra: some conceptual and mathematical problems. *Sci. Mar.* **58**, 17–29.
- 28 Laws, E. A. & Archie, J. W. 1981 Appropriate use of regression analysis in marine biology. *Mar. Biol.* **65**, 13–16. (doi:10.1007/BF00397062)
- 29 Clarke, M. R. B. 1980 The reduced major axis of a bivariate sample. *Biometrika* **67**, 441–446. (doi:10.1093/biomet/67.2.441)
- 30 Finkel, Z. V. 2001 Light absorption and size scaling of light-limited metabolism in marine diatoms. *Limnol. Oceanogr.* **46**, 86–94. (doi:10.4319/lo.2001.46.1.0086)
- 31 Goldman, J. C. 1993 Potential role of large oceanic diatoms in new primary production. *Deep-Sea Res. I* **40**, 159–168. (doi:10.1016/0967-0637(93)90059-C)
- 32 Cermeño, P., Marañón, E., Rodríguez, J. & Fernández, E. 2005 Size-dependence of coastal phytoplankton photosynthesis under vertical mixing conditions. *J. Plankton Res.* **27**, 473–483. (doi:10.1093/plankt/fbi021)
- 33 Fernández, A., Mouriño-Carballido, B., Bode, A., Varela, M. & Marañón, E. 2010 Latitudinal distribution of *Trichodesmium* spp. and N₂ fixation in the Atlantic Ocean. *Biogeosciences* **7**, 3167–3176. (doi:10.5194/bg-7-3167-2010)
- 34 Menden-Deuer, S. & Lessard, E. J. 2000 Carbon to volume relationships for dinoflagellate, diatoms, and other protist plankton. *Limnol. Oceanogr.* **45**, 569–579. (doi:10.4319/lo.2000.45.3.0569)
- 35 Rivkin, R. B. & Seliger, H. H. 1981 Liquid scintillation counting for ¹⁴C uptake of single algal cells isolated from natural. *Limnol. Oceanogr.* **26**, 780–785. (doi:10.4319/lo.1981.26.4.0780)
- 36 Li, W. K. W. 1994 Primary production of prochlorophytes, cyanobacteria, and eucaryotic ultraphytoplankton: measurements from flow cytometry sorting. *Limnol. Oceanogr.* **39**, 169–175. (doi:10.4319/lo.1994.39.1.0169)
- 37 Jardillier, L., Zubkov, M. V., Pearman, J. & Scanlan, D. J. 2010 Significant CO₂ fixation by small prymnesiophytes in the subtropical and tropical northeast Atlantic Ocean. *ISME J.* **4**, 1180–1192. (doi:10.1038/ismej.2010.36)
- 38 West, G. B., Brown, J. H. & Enquist, B. J. 1997 A general model for the origin of allometric scaling laws in biology. *Science* **276**, 122–126. (doi:10.1126/science.276.5309.122)
- 39 Niklas, K. J. 1994 *Plant allometry, the scaling of form and process*. Chicago, IL: The University of Chicago Press.
- 40 Niklas, K. J. & Enquist, B. J. 2001 Invariant scaling relationships for interspecific plant biomass production rates and body size. *Proc. Natl Acad. Sci. USA* **98**, 2922–2927. (doi:10.1073/pnas.041590298)
- 41 Dodds, P. S., Rothman, D. H. & Weitz, J. S. 2001 Re-examination of the ‘3/4-law’ of metabolism. *J. Theor. Biol.* **209**, 9–27. (doi:10.1006/jtbi.2000.2238)
- 42 Bokma, F. 2004 Evidence against universal metabolic allometry. *Func. Ecol.* **18**, 184–187. (doi:10.1111/j.0269-8463.2004.00817.x)
- 43 Isaac, N. J. B. & Carbone, C. 2010 Why are metabolic scaling exponents so controversial? Quantifying variance and testing hypothesis. *Ecol. Lett.* **13**, 728–735. (doi:10.1111/j.1461-0248.2010.01461.x)
- 44 Finkel, Z. V., Irwin, A. J. & Schofield, O. 2004 Resource limitation alters the 3/4 size scaling of metabolic rates in phytoplankton. *Mar. Ecol. Prog. Ser.* **273**, 269–279. (doi:10.3354/meps273269)
- 45 Raven, J. A. 1998 The twelfth Tansley Lecture. Small is beautiful: the picophytoplankton. *Func. Ecol.* **12**, 503–513. (doi:10.1046/j.1365-2435.1998.00233.x)
- 46 Sunda, W. G. & Hardison, D. R. 2010 Evolutionary trade-offs among nutrient acquisition, cell size, and grazing defense in marine phytoplankton ecosystem stability. *Mar. Ecol. Prog. Ser.* **401**, 63–76. (doi:10.3354/meps08390)
- 47 Verdy, A., Follows, M. & Flierl, G. 2009 Optimal phytoplankton cell size in an allometric model. *Mar. Ecol. Prog. Ser.* **379**, 1–12. (doi:10.3354/meps07909)
- 48 Thingstad, T. F. & Sakshaug, E. 1990 Control of phytoplankton in nutrient recycling ecosystems. Theory and terminology. *Mar. Ecol. Prog. Ser.* **63**, 261–272. (doi:10.3354/meps063261)
- 49 Stolte, W. & Riegman, R. 1995 Effect of phytoplankton cell size on transient-state nitrate and ammonium uptake kinetics. *Microbiology* **141**, 1221–1229. (doi:10.1099/13500872-141-5-1221)
- 50 Chisholm, S. W. 1992 Phytoplankton size. In *Primary productivity and biogeochemical cycles in the sea* (eds P. G. Falkowski & A. D. Woodhead), pp. 213–236. New York, NY: Plenum Press.
- 51 Naselli-Flores, L., Padisak, J. & Albay, M. 2007 Shape and size in phytoplankton ecology: do they matter? *Hydrobiologia* **578**, 157–161. (doi:10.1007/s10750-006-2815-z)
- 52 Thingstad, T. F., Øvreås, L., Egge, J. K., Løvdal, T. & Heldal, M. 2005 Use of non-limiting substrates to increase size; a generic strategy to simultaneously optimize uptake and minimize predation in pelagic

- osmotrophs? *Ecol. Lett.* **8**, 675–682. (doi:10.1111/j.1461-0248.2005.00768.x)
- 53 Villareal, T. A., Joseph, L. & Brzezinski, M. A. 1999 Biological and chemical characteristics of the giant diatom *Ethmodiscus* (Bacillariophyceae) in the central North Pacific gyre. *J. Plankton Res.* **35**, 896–902. (doi:10.1046/j.1529-8817.1999.3550896.x)
- 54 Foster, R. A., Kuypers, M. M. M., Vagner, T., Paerl, R. W., Musar, N. & Zehr, J. P. 2011 Nitrogen fixation and transfer in open ocean diatom-cyanobacterial symbioses. *ISME J.* **5**, 1484–1493. (doi:10.1038/ismej.2011.26)
- 55 Irwin, A. J., Finkel, Z. V., Schofield, O. M. E. & Falkowski, P. G. 2006 Scaling-up from nutrient physiology to the size-structure of phytoplankton communities. *J. Plankton Res.* **28**, 459–471. (doi:10.1093/plankt/fbi148)
- 56 Li, B.-L., Gorshkov, V. G. & Makarieva, A. 2004 Energy partitioning between different-sized organisms and ecosystem stability. *Ecology* **85**, 1811–1813. (doi:10.1890/03-0693)
- 57 del Giorgio, P. A. & Duarte, C. M. 2002 Respiration in the open ocean. *Nature* **420**, 379–384. (doi:10.1038/nature01165)
- 58 Armstrong, R. A. 1999 Stable model structures for representing biogeochemical diversity and size spectra in plankton communities. *J. Plankton Res.* **21**, 445–464. (doi:10.1093/plankt/21.3.445)
- 59 Thingstad, T. F. 1998 A theoretical approach to structuring mechanisms in the pelagic food web. *Hydrobiologia* **363**, 59–72. (doi:10.1023/A:1003146310365)
- 60 Finkel, Z., Beardall, J., Flynn, K. J., Quigg, A., Rees, T. A. V. & Raven, J. 2010 Phytoplankton in a changing world: cell size and elemental stoichiometry. *J. Plankton Res.* **32**, 119–137. (doi:10.1093/plankt/fbp098)
- 61 Arrigo, K. R. 2005 Marine microorganisms and global nutrient cycles. *Nature* **437**, 349–355. (doi:10.1038/nature04159)